Int.J.Nano Dim.2(2): 85-103, Autumn 2011
ISSN: 2008-8868

Contents list available at **IJND**

International Journal of Nano Dimension

Journal homepage: *www.IJND.ir*

Review

Synthesis and characterization of barium strontium titanate (BST) micro/nanostructures prepared by improved methods

M. Enhessari[1,*]
A. Parviz[1]
K. Ozaee[3]
H. Habibi Abyaneh[4]

[1]Department of Chemistry, Naragh Branch, Islamic Azad University, Naragh, Iran.
[2]Young Researchers Club, Naragh Branch, Islamic Azad University, Naragh, Iran.
[3]Department of Chemistry, Payame Noor University, Delijan, Iran.

Received: 03 April 2011
Accepted: 24 June 2011

* Corresponding author:
M. Enhessari
Department of Chemistry, Naragh Branch, Islamic Azad University, Naragh, Iran.
Tel +98 866 4463920
Fax+98 866 4463920
Email enhessari@gmail.com

ABSTRACT

Nowadays various methods are presented for synthesis of barium strontium titanate (BST) nanopowders with different morphology and properties. Each of these (BST)s has got individual characterization that makes it suitable for a special application. Every method has a special quality, causes it to have preference over the other methods. Low processing temperature is a desired point which most of methods are aimed to reach. Below are some BST properties and fabrication routes summarized.
X-ray diffractometer is used to investigate the characterization of synthesized BST and in some methods analysis of electron microscopy and Energy Dispersive X-Ray Spectroscopy are provided.

Keywords:*barium Strontium titanate ($Ba_{1-x}Sr_xTiO_3$, BST); Nanostructures*

INTRODUCTION

In recent years, increasing attention has been paid to the synthesis and characterization of nanomaterials because of their novel chemical and physical properties arising from the large surface–volume ratios and also the quantum size effect, compared with those of bulk counterparts [1-5]; similarly barium strontium titanate ($Ba_{1-x}Sr_xTiO_3$, BST) ferroelectric materials have attracted considerable attentions due to their chemical stability, high permittivity, high tunability and low dielectric losses [6]. The physicochemical properties of these nanomaterials are highly sensitive to their size, shape, and composition [7]. It is well-known that BST has a variety of electronic applications in multilayer and voltage-tunable capacitors, dynamic random access memories (DRAM), microwave phase shifters, tunable filters, oscillators, uncooled infrared sensors, etc. due to the high dielectric constant, nonlinear variation of dielectric constant with the electric field, ferroelectricity, pyroelectric properties and so on [8-17].

These aforementioned properties strongly depend on the composition and characteristics of raw materials [7]. Ferroelectric materials have shown huge potential for microwave applications as tunable devices [18]. Barium strontium titanate (BST), are the most extensively investigated materials to date because of their high tunability and low dielectric losses at room temperature [19]. Ferroelectric materials have been extensively studied in thin film form, mainly for the application as multilayer ceramic capacitors (MLCCs) and the dynamic random access memories (DRAM) [20]. Among the many types of ferroelectric materials, the barium strontium titanate (BST) has been the most intensively investigated because of its high dielectric constant, low dielectric loss and good thermal stability [21-24]. Moreover, the temperature range in which the ferroelectric behaviour is reflected can be easily controlled by adjusting the barium-to-strontium ratio [20].The properties of nanostructures differ from that of bulks due to the small sizes and large surface-to-volume ratios [20]. However BST powders were commonly prepared by solid-state reaction [25,26] sol–gel [27], and hydrothermal methods [28] until 2006. Various innovative approaches, like spray pyrolysis [29], combustion synthesis [30,31], chemical co-precipitation [32,33], pulsed laser deposition (PLD), r.f. sputtering, chemical vapour deposition (CVD), electrochemical [34], electrostatic spray assisted vapour deposition (ESAVD) [35], have been used to synthesize BST powders [14. Various chemical methods have been studied to obtain different shapes and forms, such as rods, wires, drums and cubes, etc. by using suitable capping agents during the synthesis [36,37]. The solid-state technique requires a calcination step at high temperature to produce a crystalline solid solution, and it can be contaminated due to the repeated grinding. The obtained powder particles are usually big in size and wide in range [38,39]. The sol–gel technique is capable of producing nano-sized powders, but most of the starting chemicals are expensive, sensitive to moisture, and require a particular processing environment to control the properties. The powder produced is normally amorphous [40, 41]. Unlike both techniques, the hydrothermal technique is able to produce nano-crystalline powders at low temperature (as low as 80°C); the powder particle size range is small, and the method is relatively inexpensive [42-44]. However, it is hard to control the stoichiometry of the final products produced by this technique [45]. However, in the hydrothermal process, impurities could be introduced for the adoption of mineralizers such as NaOH or KCl. Hence, the sol–gel or sol-precipitation route become more and more popular for the preparation of high purity BST and other perovskite oxide powders [34]. Most of the powders show equiaxial or quasi-spherical morphology from either solid-phase synthesis or wet chemical synthesis method [14]. Both PLD and r.f. sputtering yield high-quality films but these techniques are relatively expensive due to the ultrahigh vacuum (UHV) requirements. On the other hand, chemical techniques are cheaper and often more compatible with the industrial processing. However, CVD and sol–gel techniques tend to use organometallic precursors, which normally have problems with the elimination of residual organic parts in the deposited films, even after post heat treatment [35]. ESAVD has several advantages over conventional deposition techniques, such as high deposition efficiency, direct deposition under ambient atmosphere, easy control of surface morphology of the deposited layers and flexibility to coat complex shaped engineering components with good conformal coverage [46,47]. Barium titanate ($BaTiO_3$) and Strontium titanate ($SrTiO_3$) are crystallined in perovskite structure. Figure 1 shows the perovskite structure for $BaTiO_3$. When $SrTiO_3$ is added to $BaTiO_3$, Ba ions can be replaced with Sr ions lead to form the BST in the mentioned structure.

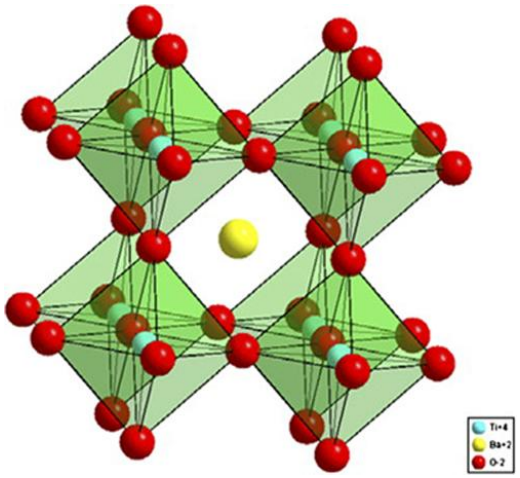

Fig.1. Perovskite structure [47].

SYNTHESIS AND CHARACTERIZATION

Direct large-scale synthesis of perovskite barium strontium titanatenano-particles from solutions

Among synthesis techniques, wet chemical method, which is usually inexpensive, can be conducted at low temperatures and yet offers good compositional and structural control of the products. This is particularly suitable for making nano-structured ferroelectric oxides [13]. In a wet chemical processing, temperature and pressure are the two factors that have critical influences on the structure and property of the products [13]. A higher temperature and pressure may improve the crystallinity of the nano-structures but also lead to a higher level of processing inconvenience and more difficulties in the size control of the products [13,20]. In this study, crystallized BST nano-particles were obtained by using J.Q. Qi et al.'s technique of which the processing temperature did not exceed 60°C [13]. The starting materials for the synthesis included high purity $Ba(OH)_2$-$8H_2O$, $Sr(OH)_2$-$8H_2O$, $Ti(OBu)_4$ and deionized water (DIW). The first step was to separately prepare a base solution and a titanium solution. The second step was to allow the reaction to take place by dripping the titanium solution into the base solution (60°C) under vigorous stirring. An instantaneous formation of white precipitation was observed. The white precipitation was obtained by filtration and baked at 60°C for 24 h in an oven [13]. Using the nano-particles, BST ceramics were prepared via a simplified ceramic processing. Elemental ICP analysis of the powders has revealed the atomic ratio Ba:Sr:Ti is in good consistence with that in the start compositions, indicating a good compositional control of this method. As shown in XRD pattern (Figure 2) except for one small peak appearing at about 24°, all other peaks are identified as formed perovskite BST. The peak sharpness and intensity indicate that BST is well crystallized. The post-synthesis annealing has strong influence on the lattice symmetry of the nano-particles [13]. A microstructural factor that possibly affects the lattice symmetry is interstitial hydrogen. Having been synthesized from an aqueous solution, the particles are expected to contain hydrogen that may exist in the interstitial sites of BST lattices [13]. Observations by X-ray diffraction, scanning electron microscopy and transmission electron microscopy TEM indicate that the particles are well-crystallized, chemically stoichiometric and ~50 nm in diameter [13]. Obviously the low synthesis temperature is the main reason for the formation of dislocations observed in the lattice. Further experiments have indicated that the particle size can be controlled through modifying the solution concentration, the synthesis temperature, the stirring rate and/or the drying temperature. For example, finer particles can be obtained in thinner solution. The BST nano-particles prepared by this process are very useful for making high-quality ceramics and composites [13]. The ferroelectric behaviors of BST ceramics made from these nano-particles were characterized. As shown in Figure 3, the ceramics show typical ferroelectric hysteresis loops that are analog to that of regularly prepared ceramics in terms of the values of the polarization and coercive field. BST ceramics with other compositions were also prepared by a similar processing and excellent dielectric and ferroelectric properties were obtained [13]. The nano-particles can also be used in the fabrication of other useful structures, such as BST/MgO core-shell structures for microwave components [48].

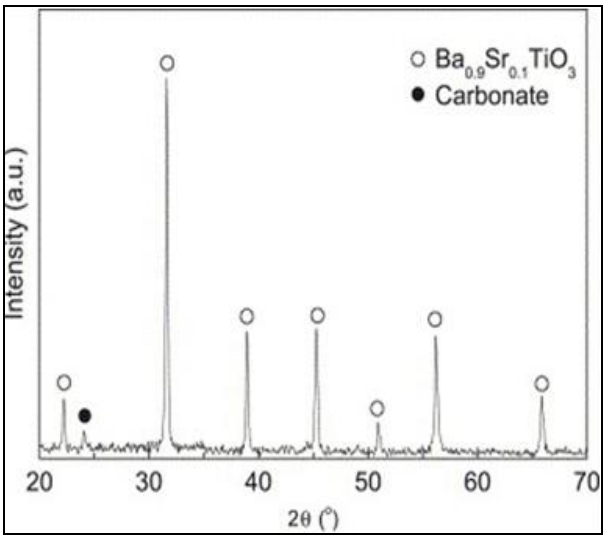

Fig.2. X-ray diffraction pattern of $(Ba_{0.9}\ Sr_{0.1})TiO_3$nano-particles[13].

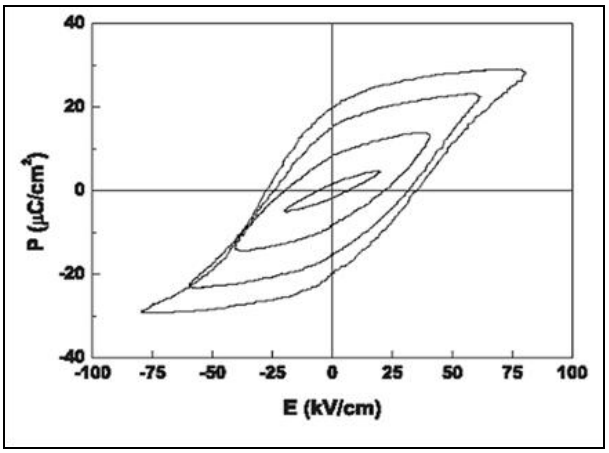

Fig.3. Ferroelectric hysteresis loops of BST ceramics made from the nano-particles via a simplified ceramic processing [13].

Barium strontium titanatenanocrystalline thin films prepared by soft chemical method

The electrical properties of BST materials are closely linked to their microstructural feature and fabrication process [49-52].Their manufacturing technology is known to have a strong effect on the structural and properties of ceramics and thin films: the size and shape of grains, the domain size and the atomic structure of grain boundaries. A factor which has critical influence on the structure and property of the materials is the temperature of heat treatment [20]. BST nanocrystalline thin films were prepared by soft chemical method and crystallized in a short time and lower temperature of heat treatment using a microwave oven. Flow chart describing the $Ba_{0.65}Sr_{0.35}TiO_3$ precursor solution and thin film processing is showed in Figure 4. Titanium (IV) isopropoxide (AlfaAesar, 99.999% purity), barium carbonate (Aldrich, 99.999% purity), strontium carbonate (Aldrich, 99.9% purity), ethylene glycol (Labsynth, 99.5% purity) and citric acid (Merck, 99.9% purity) were used as raw materials [20]. Finally the films were crystallized at 600, 650 and 700°C for 15 min in a domestic microwave oven using a SiC susceptor, which absorbs the microwave energy and rapidly transfers the heat to the film. No post annealing treatment was performed after crystallization. The desired thickness was obtained by several cycles of deposition and annealing treatment. Even at 600°C the film displayed a well-crystallized perovskite phase. No significant changes were observed as the temperature rose to 700°C. The films were polycrystalline without preferential orientation, and no secondary phase was detected. The films which were treated for 15 min in the microwave oven at 650 and 700°C, showed a nanograin size structure even when treated at 700°C. However, as the temperature increased to 700°C, the grain size range increased from 16-35 nm to 60–80 nm and the surface roughness increased from 5.0 to 8.1 nm [20].

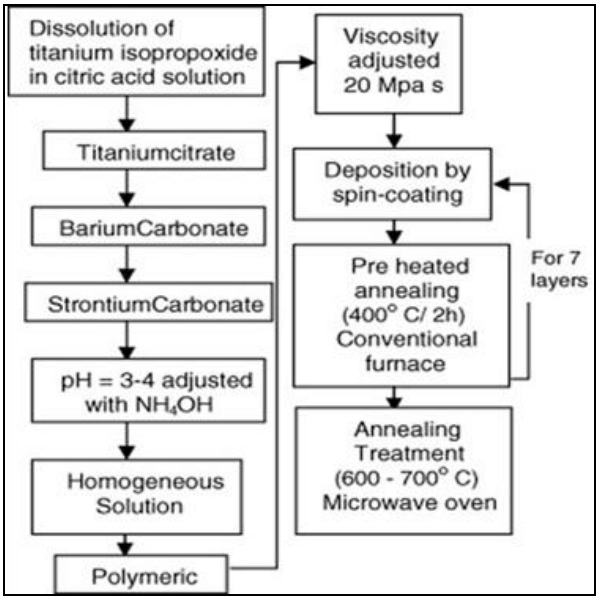

Fig.4. Flow-chart illustrating the procedure for the preparation of Ba0.65Sr0.35TiO3 precursor solutions and thin films [20].

The dielectric constant and dissipation factor as function of the frequency values of the $Ba_{0.65}Sr_{0.35}TiO_3$ thin films were measured which in the metal-BST-metal configuration with the films sandwiched between the bottom platinum and top gold electrodes, were higher than that of BSTs prepared by previous methods [20].Dielectric material for DRAM applications should have a high charge storage density and a low leakage current density. The charge storage density Q_c of $Ba_{0.65}Sr_{0.35}TiO_3$ thin film was estimated based on the following relationship (equation 1):

$$Q_c = \varepsilon_0 \varepsilon_r E \qquad \text{eq.1}$$

Where E is the applied electric field, ε_0 the vacuum permitivity, and ε_r is the dielectric constant of the $Ba_{0.65}Sr_{0.35}TiO_3$ film. The charge storage

density as a function of applied voltage is shown in Figure 5. For this relatively great thickness, the charge storage densities are suitable for use in trench type 64Mb (1–5 μC/cm^2) and 256Mb (2–11μC/cm^2) DRAMs [20].

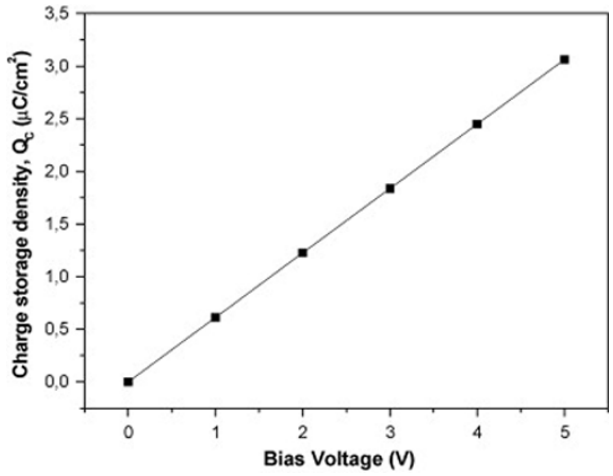

Fig.5. Charge storage density as a function of applied voltage [20].

Oxalate precursor route

Chemical co-precipitation method has attracted special interesting due to its simple procedure and low reaction temperature [6]. Barium strontium titanyl oxalate (BSTO) [$Ba_{1-x}Sr_xTiO(C_2O_4)_2.4H_2O$] is one of the important molecular precursor [53,54] for the production of BST powders with satisfying physical and chemical characteristics [6].

Quantitative ammonia into a precursor solution containing stoichiometric quantities of Ba and Sr ions was added before the co-precipitation procedure. A simple oxalate co-precipitation method based one-step cation-exchange reaction between the stoichiometric solutions of oxalotitanic acid (HTO) and barium + strontium nitrate is investigated successfully for the quantitative precipitation of Barium strontium titanyl oxalate (BSTO): $Ba_{0.6}$ $Sr_{0.4}$ $TiO(C_2O_4)_2.4H_2O$ precursor powders .see the following equation:

$$H_2TiO(C_2O_4)_2\,(HTO) + 0.6\,Ba^{2+} + 0.4\,Sr^{2+} \rightarrow Ba_{0.6}Sr_{0.4}TiO\,(C_2O_4)_2.4\,H_2O\,(BSTO)\downarrow + 2\,H^+$$

The pyrolysis of BSTO in air produced the homogeneous BST powders [6], according to the following equation:

$$Ba_{0.6}Sr_{0.4}TiO\,(C_2O_4)_2.4\,H_2O\,(BSTO) + O_2 \rightarrow Ba_{0.6}Sr_{0.4}TiO_3\,(BSTO) + 4\,CO_2 + 4\,H_2O$$

According to Schrey [32], the pH value appears to be the key factor in the transformation of existing state of titanium [6]. In order to prevent the formation of TiO_2 and obtain single phase of BST, the very stringent control of pH of 2.5–3.5 is required during the precipitation. Single phase of BST can be obtained provided that the final pH (after being stirred at 80°C for 2 h) of resulting reaction mixture is in the range 2.5–3.0 [6].

To investigate the thermal degradation behaviors of the $Ba_{0.6}$ $Sr_{0.4}$ $TiO(C_2O_4)_2.4H_2O$ (BSTO) powders, TGA/DSC analyses were carried out in static air in the temperature range of RT to 1000°C. It can be inferred from the TG curve that the reaction ended at about 750°C. A further increase in the sintering temperature promoted crystallization of BST, but no new chemical reactions took place. As the result indicated, the precursor was calcined at 800°C to make the pyrolysis of BSTO go to its completion and obtain BST powders with complete crystallization [6].

Figure 6 shows the XRD patterns of BST powders obtained by the pyrolysis of BSTO at 800°C/4h in air. The peaks corresponding to impurity appear only when the final pH value (after stirred for 2 h 80°C) deviates from the range 2.5–3.0. A careful analysis of the XRD pattern (Figure 7) shows that all the peaks corresponding to only BST are present and the peaks perfectly match with the standard pattern. It is clear that the pattern, shown in Figure 7, illustrates the presence of all reactions corresponding to only BST. This further confirms the formation of only BSTO rather than the other oxalates by the present route. The co-precipitation of Ba and Sr is nearly completed to reach the right Ba/Sr ratio [6].

The co-precipitation of Ba and Sr is nearly completed to reach the right Ba/Sr ratio [6]. From all the results above, it could be assuredly concluded that single phase of $Ba_{0.6}$ $Sr_{0.4}$ TiO_3 powders were successfully prepared by the present chemical co-precipitation method [6].

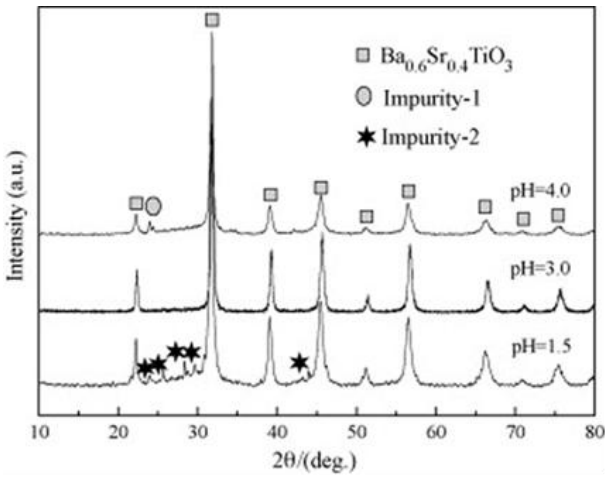

Fig.6. XRD patterns of BST powders from BSTO obtained at different pH value. [6]

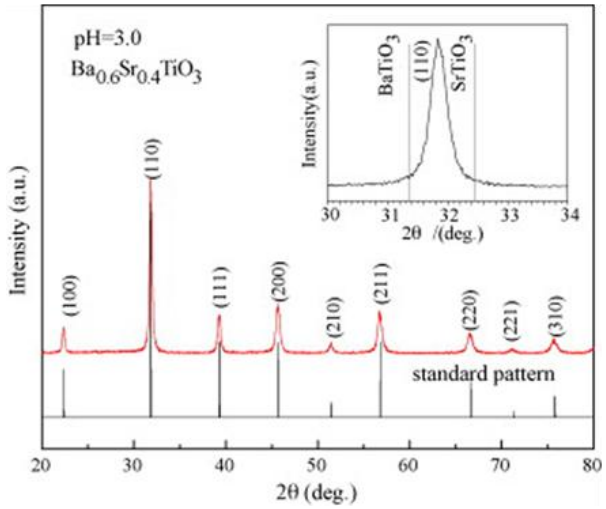

Fig.7. XRD patterns of BST powders. [6]

Figure 8 shows the SEM photograph of BST powders. The particles of BST are spherical in nature with sizes in the range of 0.8–1.2µm and are agglomerated. Further, the spherical BST particles showed distinct brain-like morphology with rough surface. It seems that every BST particle is the conglomeration of numerous grains; but the hypothesis can be rejected easily only if we take the particle size of BSTO and BST powders into consideration; (BSTO particles are of spherical type with sizes in the range of 1–1.5µm [6]). The special shape of BST comes into being during the calcining process with pyrolysis of BSTO and release of CO_2. The BST powders obtained from the present route are expected to have good sintering activity since they possess sub-micron powder particle size and surface area of nano-powders. The sintering activity of ceramic powders becomes higher as the surface area increases [6].

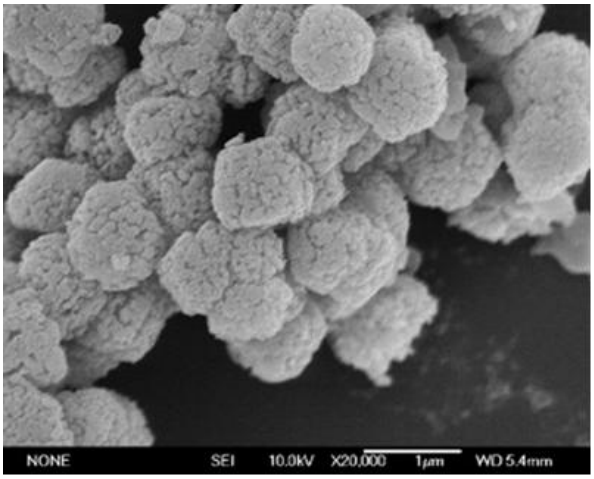

Fig.8. SEM photographs of BST powders. [6,14]

The BSTO and BST powders obtained by aforementioned technique without dispersants were homogeneous with quasi-orbicular morphology. Two kinds of dispersants namely ammonium salt of poly methacrylic acid (PMAA-NH4) and polyethylene glycol (PEG) were added respectively during the co-precipitation procedure. The particles grew into spindle shape with the effect of PEG (Figure 9) [14].

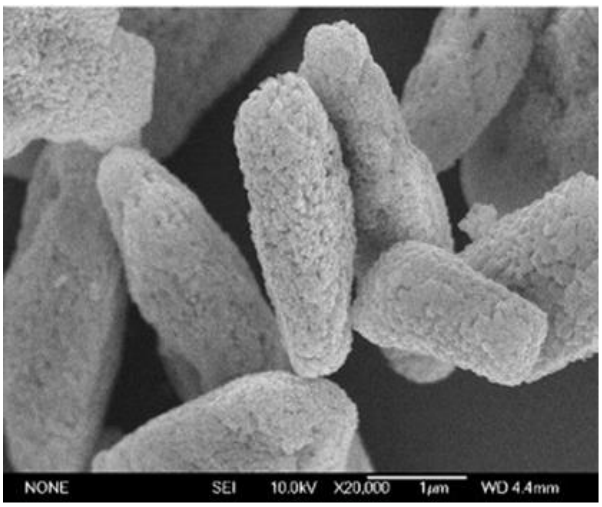

Fig.9. SEM images of surface of BST powders, with PEG [14]

During the co-precipitation step, the dispersants worked to form composite crystal nucleus with special morphology and the growth of the composite crystal nucleus formed the special shaped particles. The addition of PEG or PMAA-NH_4 does not affect the phase compositions of the ultimate BST powders [14].

In addition, it was reported by Khollam et al. [55] that star-shaped barium–strontium titanate powders could be obtained through oxalate co-precipitation method using in-situ $C_2O_4^{2-}$ ions as capping agent to induce the growth of the BST grains [14].

Composition and shape control of BST nanocrystals via a solvothermal route

Barium titanate ($BaTiO_3$) and its related compounds are among the significant dielectric materials of major interest for their applications in electronic ceramics. When barium was substituted with strontium, forming solid solutions of barium titanate and strontium titanate, collectively known as barium strontium titanate ($Ba_{1\_x}Sr_xTiO_3$, x=0–1, BST), the Curie temperature can be easily tuned by changing the $SrTiO_3$ content. To achieve fine microstructure and high performance, it is necessary to start with the synthesis of fine, stoichiometric and highly dispersed powders with narrow size distribution [7].

In this part, well-dispersed and shaped-composition-controlled $Ba_{1\_x}Sr_xTiO_3$ (x=0–1) nanocrystals using the mixture of ethylenediamine and ethanolamine as the solvent have been synthesized via the solvothermal route. $Ba_{1\_x}Sr_xTiO_3$ samples with x = 0, 0.3, 0.5, 0.8, and 1.0 (denoted sample S1, S2, S3, S4, and S5, respectively) were synthesized by the solvothermal method using barium acetate ($Ba(CH_3COO)_2$), strontium nitrate ($Sr(NO_3)_2$) and tetrabutyltitanate ($Ti(OC_4H_9)_4$) as precursors. The crystallinity and structure of the five solvothermally synthesized BST samples were examined using XRD. All diffraction peaks can be assigned to a cubic perovskite structure [7].

All the samples are not phase separated (barium-rich and strontium-rich phases), regardless of the Ba/Sr molar ratio in samples [56]. Lattice constants and Ba/Sr mole ratios are gradually decreased from sample S1 to S5. Additionally, the peak intensity is found to be increased with increasing strontium content in BST, suggesting the improved crystallinity with strontium substitution [7].It is evident that all samples consist of well-dispersed nanoparticles without large hard aggregations and that both the morphology and size of the particles depend on the product composition. The particle morphology changes from irregular sphere to polygon and to cube as the strontium content increases in BST powders [7]. The final particle morphology is probably a competitive result of crystallographic growth and preferential dissolution of high-energy faces [57].

The particle sizes (DTEM) evaluated from TEM images are 15, 10, 30, 31, and 36nm for samples S1, S2, S3, S4, and S5 respectively, suggesting that the as-synthesized nanoparticles are mostly monocrystalline without aggregates of nanosized subunits. The increase in particle size with the increase of strontium proportion in BST samples is probably due to the different growth rate with different strontium proportions in the product, because the solvent molecules have a stronger binding force to barium than to strontium [7].

The single-phase solid solution nature of all five samples, the Ba/Sr molar ratios of BST samples are different from that in initial reactants. But the trends are the same, that is, the Ba/Sr molar ratio decreases as the x value increases, indicating that strontium is preferentially incorporated into the BST [7]. The preferential incorporation of strontium into BST can be explained based on the following two facts: the formation of $SrTiO_3$ is thermodynamically more favorable than $BaTiO_3$, and the $SrTiO_3$ is more stable than $BaTiO_3$ at lower M cations concentration (M= Sr and Ba) and lower reaction temperature [56].

The standard Gibbs energy of formation for Sr^{2+}cations is more negative than that for Ba^{2+}, and hence the Sr^{2+} species have higher reactivity to react with titanium preferentially, resulting in the higher strontium proportion in final products [7].

The 2-D lattice fringers clearly illustrate that the nanoparticles are crystalline without defect structure such as dislocations or grain boundaries, further confirming the monocrystalline nature of the solvothermally synthesized BST nanoparticles [7]. The lattice plane spacings for samples S1, S3, and S5 are calculated to be 2.84, 2.79, and 2.76Å respectively, to the (110) plane of the cubic perovskite structure of BST materials [58]. The lattice spacing clearly decreases with the increasing strontium proportion in the BST samples, due to

the smaller diameter of Sr^{2+} ions relative to Ba^{2+} ions [7]. It is proposed that when the aqueous solution of KOH was added into the flask, the $Ti(OH)_4$ precipitate dissolved and the $Ti(OH)_6^{2-}$ species came to existence [7] . The forming of BST based on the reaction of Ba^{2+} and Sr^{2+}cations with $Ti(OH)_6^{2-}$ was studied under a high basic condition [59].Below is the summarized reaction equation:

$$(1-x)Ba^{2+} + x\,Sr^{2+} + Ti(OH)_6^{2-} \rightarrow Ba_{1-x}Sr_xTiO_3 + 3\,H_2O$$

In the present solvothermal synthesis, the stoichiometric initial molar ratio of barium and strontium, relative to titanium, without any other additive could lead to the single solid solution of BST [7]. It is expected that the low-temperature procedure, which does not require demanding conditions, could facilely scale-up the synthesis of the perovskite nanostructures [7].

Barium strontium titanate powders prepared by spray pyrolysis

The traditional method of preparation of BST by solid state reaction, from $BaCO_3$ or BaO, SrO and TiO_2, is not suitable for preparation of ceramics for high performance application because the material shows large particle size, nonhomogeneity and presence of impurities [60]. The possible solution of these problems is the application of some chemical methods in preparation of BST powders, for example, sol–gel, coprecipitation, hydrothermal or spray pyrolysis [61]. Spray pyrolysis is a promising technique for producing various materials in a wide range of composition, size and morphology. Powders and films can be successfully prepared [62].The powders characterization confirms that powders are composed of spherical submicronic particles with internal nanocrystalline structure [63].

Spray pyrolysis involves passing an aerosol of a precursor solution through a graded temperature reactor, in which the individual droplets are thermally decomposed to form the oxide particles [61]. The aerosols may be generated by pneumatic or ultrasonic nebulizer [64].

In this work, the precursor solution for BST ($Ba_{0.8}Sr_{0.2}TiO_3$) was prepared starting from titanium citrate, barium acetate and strontium acetate. Stoichiometric amount of strontium and barium acetate were dissolved in water and two solutions were mixed together [63].

Ultrasonic nebulizer of 2.5MHz was used for aerosols generation. It is important to avoid the formation of carbonates during the synthesis of BST. It is well known that strontium and barium carbonates easily form in sol–gel processes when the organic precursor is used. This carbonate is very difficult to eliminate after the thermal treatment. Since the carbonate forms at temperatures lower than temperature of BST formation it was necessary to perform fast heating of the aerosol. On the other hand, high heating rate can result in formation of porous particles or particles with volcanic structure. To obtain dense particles, without carbonate, it was necessary to optimize temperature and heating rate of thermal treatment (temperature at the first chamber of the furnace, 750 ℃; temperature at the second chamber of the furnace, 600 ℃).The powder mixture was prepared from 47.95 wt.% of BST and 52.05 wt.% of SiO_2 [63].Results of X-ray diffraction analysis showed that almost single phase BST powder, with traces of carbonate (Figures 10 and 11), was obtained under the optimal processing conditions. The large peak broadening suggests formation of small crystallites. Also, the high background around the (1 0 1) peak, which is the most intense one, indicates the existence of amorphous phase. This means that crystallization was not completed. Further, it was possible to observe changes in color of the sample with time. After 60 days, it became slightly darker [63].

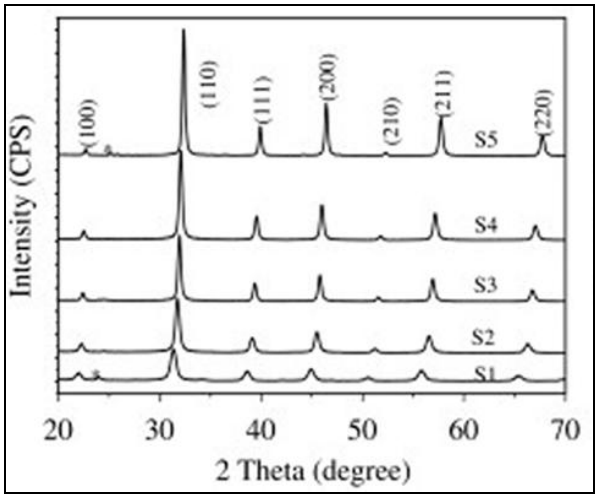

Fig.10. XRD patterns of the as-synthesized BST nanocrystal powders in the 2Θ range of 20°–70°. The asterisks marked in the figure represent the tiny by-products of carbonate [7].

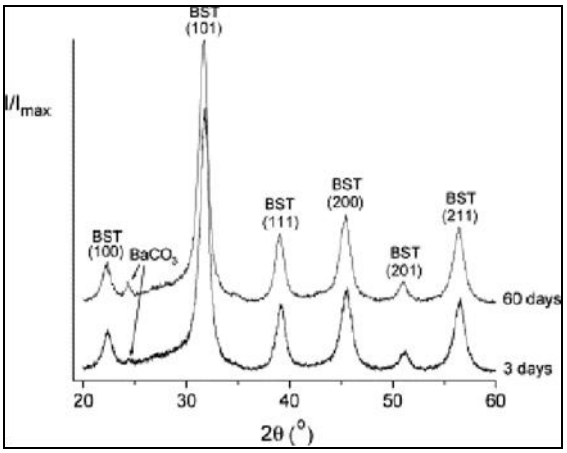

Fig.11. X-ray diffractogram of the Ba0.8Sr0.2TiO3 powder collected 3 days and 60 days after synthesis [63].

Crystallites size of BST were $\langle t \rangle$||axis-c = 9.8 nm and $\langle t \rangle \perp$axis-c = 10.8 nm [63].

SEM micrographs of the BST powders are shown at Figure12. Particles of the BST are mainly smooth and spherical, with diameter in the interval from 100 nm up to 1µm. There are no particle fragments or particles with volcanic structure. Some larger particles are rather deformed, because they are made up of several smaller droplets [63].

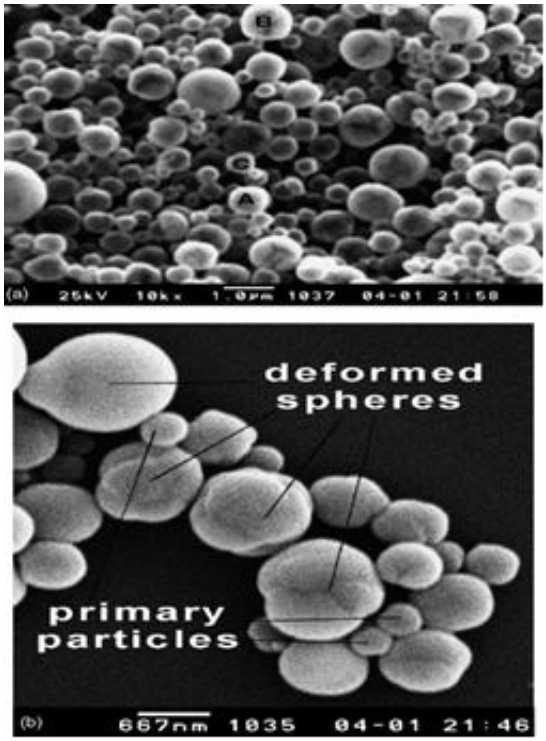

Fig.12. SEM micrographs of the BST powder: (a) general look and (b) primary particles and some larger and deformed secondary particles[63].

The morphology of the powders and densities of the particles are investigated through comparing the experimental value of the diameter with the calculated values. The theoretical diameter could be calculated according the following equation 2:

$$d = \left(\frac{cM1}{\rho}\right)^{0.33} D_0 \qquad \text{eq.2}$$

$d$is particle diameter, c solution concentration, ρ density of the BST and M_1 is molar mass of the BST. D_0, the diameter of the droplets, could be calculated according to the following equation 3[65]:

$$D_0 = 0.34\left(\frac{8\pi\gamma}{\rho f^2}\right)^{0.33} \qquad \text{eq.3}$$

Where γ is superficial tension of the solution, approximately same as of the water = 69.6 dyn/cm, ρ water density = 1 g/cm^{3}and f is frequency of the ultrasound.

In this way, the value of d_{cal} = 270 nm was obtained. This is lower value than a mean diameter of primary particles from the Figure 13b indicating hollow structure and/or microporosity of the particles [63].According to TEM results, the particles are darker at particle borders, indicating hollow structure (Figure 13a). To investigate the crystallinity, the smallest particle from Figure 13a. was magnified in Figure 13b. Under magnification (Figure13b and c), it is possible to see that material is not well crystalline in the whole particle and that there are small crystallites sized 7–13 nm inside the particle with diameter of 80 nm. Also, X-ray diffraction analysis showed the presence of the amorphous phase [63].

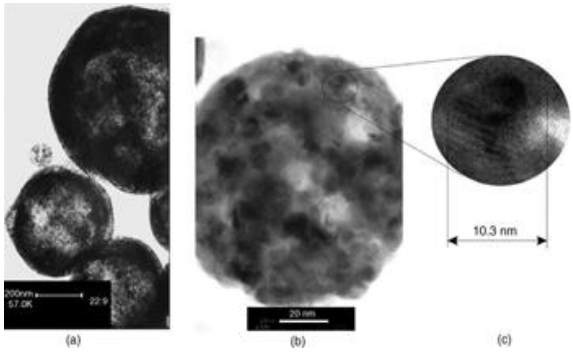

Fig.13. TEM micrographs of the BST powder [63].

Both, crystalline and amorphous parts contain the same, single phase BST [63].The crystallite size was about 10 nm [63].

The obtained powder is consisted of polycrystalline particles, with hollow structure and significant amount of amorphous phase. This is the result of high heating rate, which was inevitable to suppress formation of carbonates [63].

Barium strontium titanate thin films produced by Electrostatic Spray Assisted Vapor Deposition

The Curie temperature of $Ba_{1-x}Sr_xTiO_3$ system decreases linearly with the increasing amount of Sr in the $BaTiO_3$ lattice. Especially, BST thin films with the same concentration of Ba and Sr, namely $Ba_{0.5}$ $Sr_{0.5}$ TiO_3, are most frequently studied due to its paraelectric properties in the operating room temperature range [35].

A mixture of metal alkoxides of Ba, Sr and Ti with molar ratios of 1:1:2 has been used as the precursor solution for the deposition of BST films. Si wafers were used as substrates [46]. The applied electric field potential between the atomizer and substrate was varied in the range of 5–20 kV [35].

The BST films were deposited using ESAVD at different deposition temperatures from 400℃ to 700℃ [35].

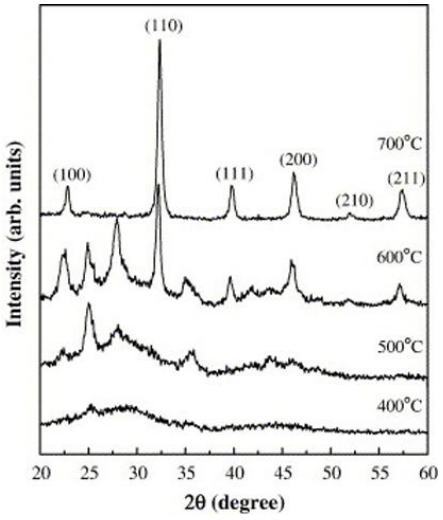

Fig.14. X-ray diffraction patterns of BST films produced by ESAVD at different deposition temperatures from 400℃ to 700℃ [46].

Figure 14 shows that the BST crystallite growth enhanced with the increase of deposition temperature and pure perovskite structure was obtained at 700℃. Below 500℃, the film is amorphous. BST films have also been deposited at low temperatures with subsequent post annealing at high temperatures in order to investigate the crystallite growth of BST.

Figure 15 illustrates the X-ray diffraction patterns of BST thin films deposited at 350℃ followed by annealing at different temperatures from 650℃ to 700℃ for 1 h. It is observed that perovskite crystalline phase appears after annealing at 650℃, however, the XRD peaks of BST films are weak and a small amount of pyrochlore phase still exists in the film. The pyrochlore phase was completely removed when the annealing temperature was increased to 675℃. As the annealing temperature was increased to 700℃, strong and sharp peaks of perovskite phase were obtained. This means that the overall crystallinity of BST thin films is enhanced with the increase in annealing temperatures [46].

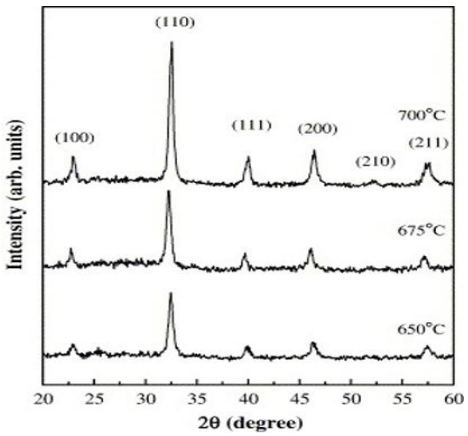

Fig.15. X-ray diffraction patterns of the BST films produced by ESAVD at 350℃ followed by annealing at temperatures from 650℃ to 700℃ for 1 h [46].

Figure 16 shows the two-dimensional and corresponding three-dimensional AFM images of the surface of the BST thin film deposited using ESAVD at 700℃. The dominant surface feature consisting of large clusters of grains is observed. The overall surface roughness is relatively high with RMS roughness of 92.8 nm [46]. It was believed that direct deposition at high temperature of 700℃ using ESAVD would cause the homogeneous gas phase reaction near the heated substrate, active intermediate species might undergo decomposition and are subjected to chemical reactions to form big grain clusters on the film surface [66].

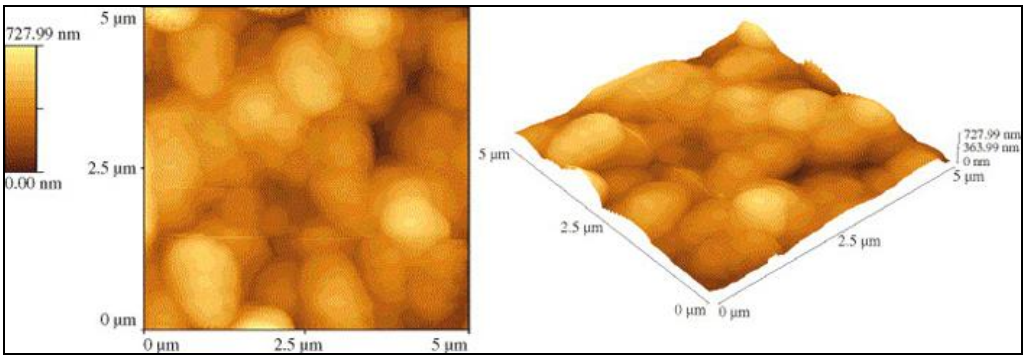

Fig.16. Two-dimensional and corresponding three-dimensional AFM images of the surface of the BST film prepared using ESAVD at 700℃ [46].

The film exhibits a well crystallized, uniform and dense microstructure consisting of a network of tightly coupled grains [46].

Figure 17 shows the cross-sectional SEM image of the BST films fabricated by ESAVD at low deposition temperature of 350℃ followed by high temperature annealing at 700℃. It reveals uniform thickness and relatively dense microstructure [46].

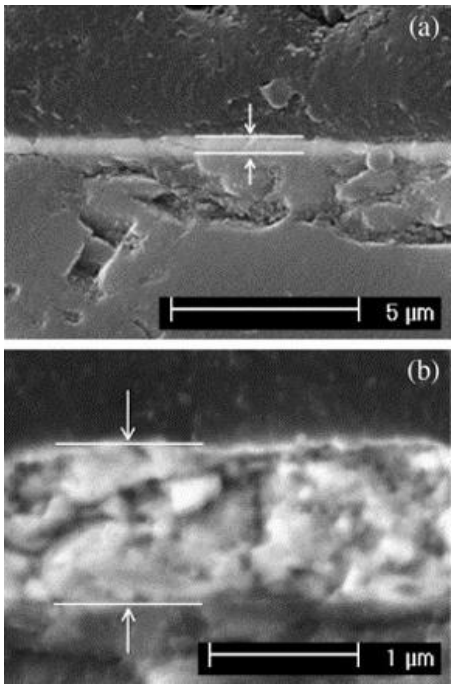

Fig.17. Microstructure of the cross-section of the BST films deposited by ESAVD at 350℃ following by annealing at 700℃ (a) under low magnification and (b) under high magnification [46].

EDX analysis of the film composition was performed and the ratio of Ba/Sr/Ti was identified to be 1.02:0.98:2, which were very close to the original starting ratios of Ba/Sr/Ti in the mixture of precursor solution [46]. With this method, high purity BST films have been obtained.

The Raman analytical results confirm the perovskite structure and paraelectric phase of the BST films at room temperature. This study demonstrates the feasibility of ESAVD to fabricate high quality BST films in an open atmosphere without the need to process in a controlled atmosphere or expensive vacuum system, which would be attractive for potential industrial fabrication [46].

Barium strontium titanate ceramics prepared by high temperature hydrothermal process

Starting materials $BaCl_2.2H_2O$ and $SrCl_2.6H_2O$ were added to distilled water containing 1.2 M of NaOH and continuously stirred at 80℃ for 2 h. The NaOH concentration was calculated based on the following chemical equations:

$$BaCl_2.2H_2O + 2\ NaOH \rightarrow Ba(OH)_2 + 2\ NaCl + 2H_2O$$

$$SrCl_2.6H_2O + 2\ NaOH \rightarrow Sr(OH)_2 + 2\ NaCl + 6\ H_2O$$

Distilled water, before the reaction, was previously boiled for 30 min to remove dissolved CO_2. The hydration water incorporated in $BaCl_2$ and $SrCl_2$ was taken into account during the preparation period to achieve a concentration of Ba + Sr = 0.6 M. Different mol ratios of Ba:Sr from 1.0:0.0 to 0.7:0.3 were used in the experiments. The solution was then filtered and mixed with different amount of TiO_2 powder (100% anatase). The concentration of anatase varied from 0.125 to 0.250 M. This gave relative concentrations of (Ba +

Sr)/TiO_2 from 4.8 (calculated as 0.6 M/0.125 M) to 2.4 (as 0.6 M/ 0.25 M). The final solution was poured into the Teflon lined pressure vessel and then placed in a pre-heated oven at 220℃ for 8–48 h. The obtained powder was filtered, washed three times using water of pH 2 adjusted by NH_4OH, filtered again and, finally, dried [45]. Finally, the prepared powders were heat treated for 2 h at 550℃ to free the incorporated water [67].

Crystal structure of the obtained samples was studied using a D8 Advance Bruker X-ray diffractometer with Cu Kα radiation. Microstructure of the powders was studied by Philips XL 30S FEG-SEM and Philips CM12 TEM. Thermogravimetric measurements were performed using Shimadzu TGA-50 [45].

It is known that hydrothermally prepared powders have a considerable amount of water incorporated in the perovskite structure [67]. Thermogravimetric analysis confirmed that the 500℃ peak, which was associated with water [67], disappeared after a heat treatment at 550℃ for 2 h [45]. The residues collected from the filter (step 2 in Figure 18) did not upset very much the initial chemical balance between Ba and Sr in the solution [45].

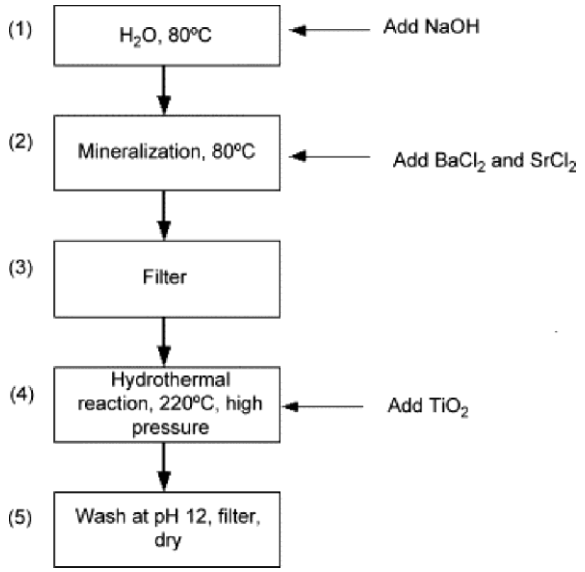

Fig.18. Flowchart of BST preparation by the high temperature hydrothermal method [45].

XRD analysis of the samples with Ba:Sr mol ratios of 0.9:0.1, 0.85:0.15, 0.8:0.2 and 0.75:0.25 (while the Ba + Sr to TiO_2 ratio for all was fixed at 2.4, and duration of the hydrothermal reaction was 16 h), showed that the compounds consisted of Ba_x Sr_{1-x} TiO_3 with two different values of x. Since the peaks of the two compounds are close to each other, fitting software was used to separate them (Figures 19 and 20) [45].

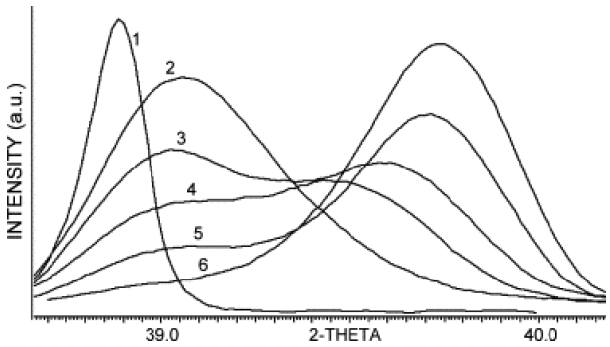

Fig.19. (1 1 1) peak of Ba-pure (1) and five samples prepared with different Ba:Sr mol ratios of 0.9:0.1 (2), 0.85:0.15 (3), 0.8:0.2 (4), 0.75:0.25 (5), and 0.7:0.3 (6). The experimental curves were smoothed for a better view [45].

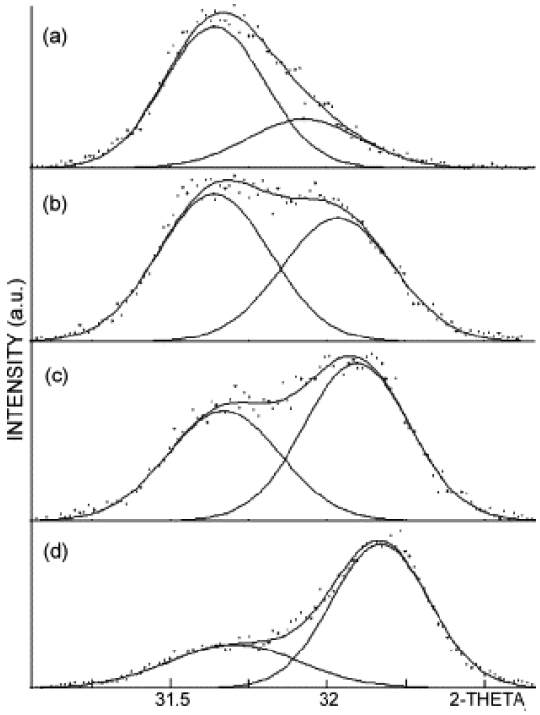

Fig.20. Spectra of (1 1 0, 1 0 1) peak of samples prepared with Ba:Sr of (a) 0.9:0.1, (b) 0.85:0.15, (c) 0.8:0.2 and (d) 0.75:0.25. Solid lines are theoretical peaks obtained from the best fit [45].

The (1 1 1) peak splits into two when %Sr increases. It is, reasonable to assume that the sample structure is not uniform and there are two

types of crystal structures, each with a different amount of Sr [45].

The grain size was calculated from the full width at half maximum (FWHM) of the peaks, using the Schrerrer's relation (equation 4):

$$t = \frac{0.9\,\lambda}{\left(B_m^2 - B_s^2\right)^{0.5}\cos\theta} \qquad \text{eq.4}$$

Where λ is the X-ray wavelength, B_m and B_s are the experimental and instrumental FWHMs values, respectively [45].

The calculated crystal size, t, is very small, in the range of 11– 20 nm, and different for the two types of crystals in the four samples with varying Ba contents. Crystal sizes calculated from (2 0 0) peak are smaller, probably because they came from the longitudinal direction, compared to the lateral direction (1 1 0, 1 0 1); and the shape of the crystals, according to the SEM pictures (see Figure 21a), is a plate-like. TEM study confirmed that the smallest particles in the powder are in the calculated range (Figure 21b). The big particles, possibly, have a complex globular structure [45].

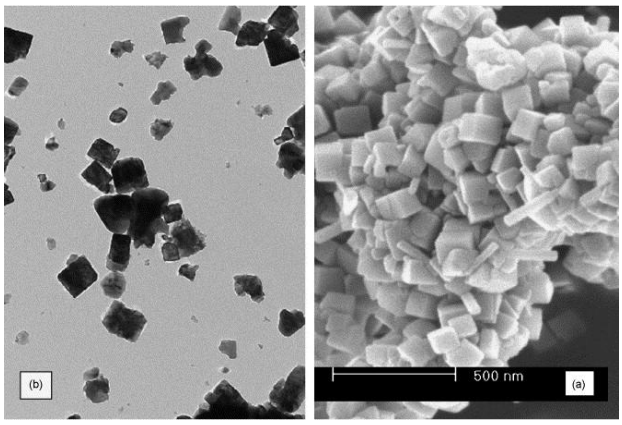

Fig.21. Micrographs of typical BST powders: (a) SEM and (b) TEM [45].

Ba losses increase with increasing of Sr content in the original mixture [45]. This behavior can be explained by a higher mobility of Sr ions compared to Ba ions [42]. If there is a small deficiency in TiO_2, then BST is a two-phase solid solution. Calculations show that when the amount of Sr in the initial solution is above 30% the final compound has a structure of more than two phases [45].

It was found that the duration of reaction did not have a great influence on the composition of the final products. Hydrothermal synthesis of barium strontium titanate at high temperature and elevated pressure showed similar results to that of a low temperature reaction [42]. Structure of the final BST product was greatly affected by two major parameters: Ba:Sr mol ratio and TiO_2 concentration. As Ba and Sr have different chemical activity and mobility, they react differently with Ti, leading to a multi-phase structure in the case of a small deficiency in Ti, and a single phase for a high deficiency in Ti. The threshold value of (Ba+Sr)/TiO_2 ratio for a single/two phase transition was about 3. The obtained phases were tetragonal $BaTiO_3$ and cubic $Ba_{0.6}Sr_{0.4}TiO_3$, if a relative share of Sr was small, less than 10%. As the amount of Sr increases it goes mostly to the cubic structure. When Sr concentration in the initial solution reaches 30%, the final BST becomes three- phased. This process is also accompanied by Ba losses [45].

Synthesis and characterization of nanocrystalline Barium Strontium Titanate powder via sol-gel processing

Barium Strontium Titanate (BST) solid solution is a strong candidate material for application in tunable ferroelectric devices. In this research, nanocrystalline BST ($Ba_{0.7}Sr_{0.3}TiO_3$) powder with average particle- diameter of 15 nm have been synthesized and characterized through a simple sol-gel process, using barium acetate, and strontium acetate and titanium isopropoxide as the precursors. In this process, stoichiometric proportions of barium acetate and strontium acetate were dissolved in acetic acid followed by refluxing, and addition of titanium (IV) isopropoxide to form BST gel. The gel was analyzed using Differential Scanning Calorimetry (DSC) and Thermal Gravimetric Analysis (TGA). The formed gel was dried at 200℃ and then calcined in the temperature range of 400 to 800℃ for crystallization (Figure 22). Phase evolution during calcination was studied using X-ray diffraction (XRD) technique. Particle size, morphology and the lattice fringes of the calcined powder were characterized by high-resolution transmission electron microscopy (HR-TEM). To study the effects of sintering on BST nanopowder, green ceramic specimens were prepared by the uniaxial compaction and then

sintered at 950–1,100℃ under atmospheric conditions. Sintered specimens were analyzed for phase composition, grain size and geometric bulk density [68].

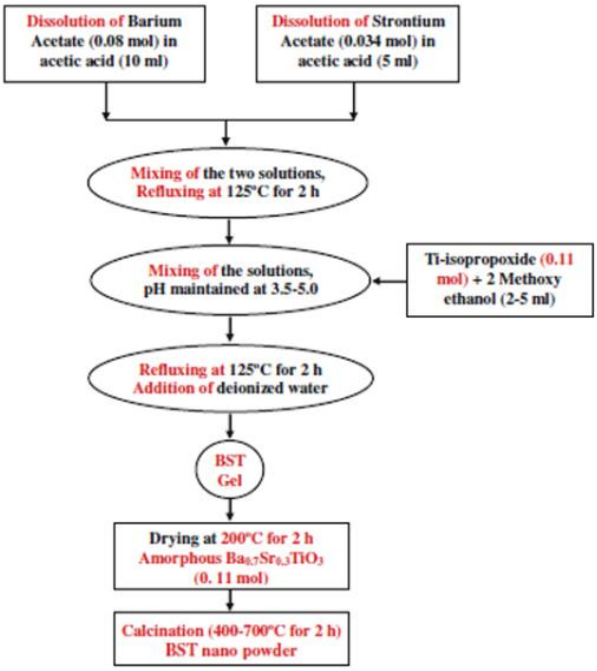

Fig.22. Schematic detailing synthesis of nanocrystalline BST powder [68]

Figure 23 shows the XRD patterns of the powder calcined in air at 600 and 700°C for 2 h, separately. It is observed that peaks obtained at 600°C are not sharp indicating that particles are not fully crystallized. Thermal heat treatment with appropriate time and temperature can cause the amorphous phase to crystallize because the amorphous phase is thermodynamically metastable state. This is what we observed, when the calcination temperature was raised from 600 to 700°C. As it was seen in Figure 23, the peaks observed for powder calcined at 700°C are sharp, revealing that the powder is fully transformed to a crystalline state at this temperature.

In both cases, the predominant phase present was $Ba_{0.7}Sr_{0.3}TiO_3$. Peaks of $Ba_{0.7}Sr_{0.3}TiO_3$ were identified using PDF card no. 00-44-0093. HR-TEM image of the as-calcined powder at 700°C is shown in Figure 24a. Crystallographic planes and ordered arrangement of atoms is visible in this image. The powder was observed to be in form of agglomerates in the dispersed solution. It was also observed that the shape of the powder was not uniform. To determine the average particle size of the powder, measurements were taken along the length and width of several particles and the average of these measurements were calculated. The average particle size of the powder was found to be ~15 nm. The particle size of the powder was also determined using the Scherrer's equation (eq.3) from the recorded XRD pattern, which was found to be ~18 nm, in line with our TEM investigation [68]. Figure 24b is a magnified TEM image showing clear lattice fringes matching the (100) lattice plane of the $Ba_{0.7}Sr_{0.3}TiO_3$ powder in cubic phase. It is well known that the lattice images are interference patterns between the direct beam and diffracted beams in HR-TEM and that the spacing of a set of fringes is proportional to the lattice spacing, when the corresponding lattice planes meet the Bragg's condition. The calculated interplanar distance from the magnified image was 0.384 nm comparing well against the standard interplanar distance of 0.396 nm for cubic $Ba_{0.6}Sr_{0.4}TiO_3$ (PDF # 00-34-0411) in [100] direction [68].

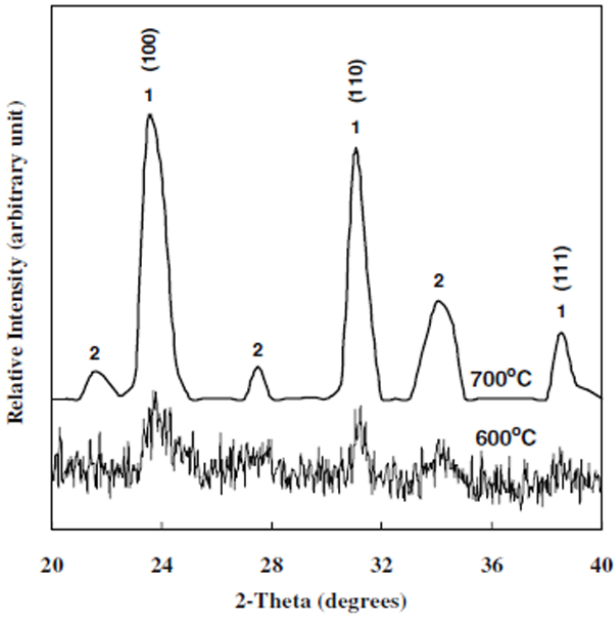

Fig.23. XRD patterns of BST nanopowder calcined at 600 and 700 °C,separately, for 2 h. Ba0.7Sr0.3TiO3 and Ba4Ti13O30 peaks, observed in these XRD traces, are marked as 1 and 2, respectively[68].

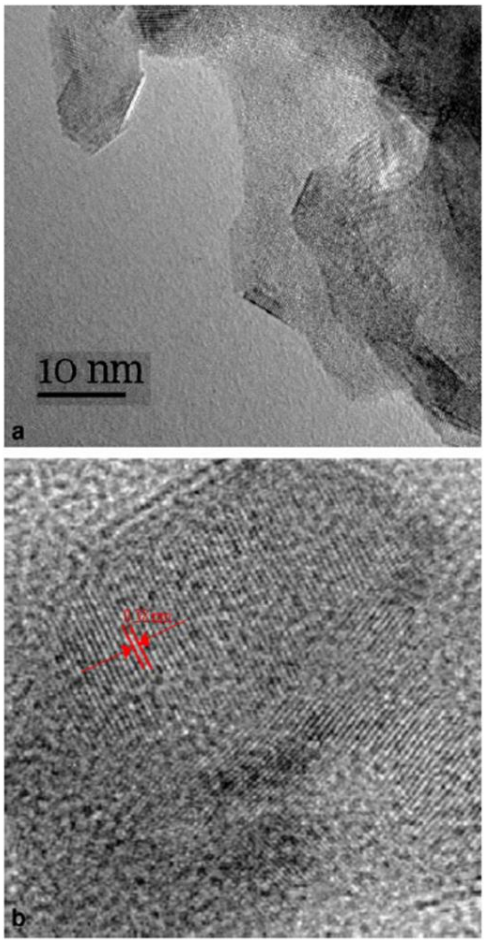

Fig.24. (a) TEM micrograph of BST powder calcined at 700°C. (b) TEM micrographs showing lattice fringes and interplanar distance (0.38 nm) of $Ba0.7Sr0.3TiO_3$ phase [68].

It was found that the carbonates of the starting chemicals react to form $Ba_{0.7}Sr_{0.3}TiO_3$ phase at around 600°C. Complete crystallization was achieved at 700°C where the phase composition is predominantly $Ba_{0.7}Sr_{0.3}TiO_3$ with a small fraction of $Ba_4Ti_{13}O_{30}$. Phase evolution, as observed in the XRD patterns were consistent with our findings on DSC analysis of the BST gel. Effects of elevated sintering temperature (950–1,100°C) on consolidated nano-BST powder were seen to have undesirable outcome—significant phase transformation occurs in this temperature range with the predominant phases being $Ba_4Ti_{13}O_{30}$ and $Sr_2Ti_5O_{12}$ and a small fraction of $Ba_{0.7}Sr_{0.3}TiO_3$. Therefore, we can conclude that it is difficult to maintain the phase purity of nano$Ba_{0.7}Sr_{0.3}TiO_3$ at elevated temperatures. The sol-gel process developed in this research can be used to deposit nano thin films of BST for their potential application in tunable ferroelectric devices [68].

CONCLUSION

Conventionally, BST compounds are prepared by the solid-state reaction of the carbonate of barium and strontium, and titanium oxide at high temperature (>1200°C) [69]. These presents the inconvenience of obtaining non-homogeneous microstructures with very large particle sizes, hard aggregates as well as high impurity contents, which is not suitable for the preparation of high-performance ceramics [7].

In the meantime, according to J.Q.Qi [13] BST nanopowders can be produced at low temperature (60°C) with a good compositional control. However dislocations are observed in these BSTs. These BSTs are useful for making high-quality ceramics and composites. The nano-particles can also be used in the fabrication of other useful structures, such as BST/MgO core-shell structures for microwave components. In this route finer particles can be obtained in thinner solution. We can achieve well crystallized and perovskite BST in single phase by the later and the first four mentioned methods. Even BST thin films obtained from electrostatic spray have perovskite structure.

Microwave energy as a rapid thermal route for the crystallization of BST films has the advantage of reducing the time and temperature of thermal treatments. It is aimed at avoiding the grain growth [20]. It is observed that dielectric constant and dissipation factor as a function of frequency in BST prepared by this route decrease in comparison with previous methods. These BSTs are suitable for use in trench type 64Mb (1–5 $\mu C/cm^2$) and 256Mb (2–11 $\mu C/cm^2$) DRAMs.

BSTs produced by simple oxalate precursor route nearly have initial Ba/Sr ratio in final composition. By this method without dispersant, homogeneous BST with brain-like feature (quasi-orbicular morphology) will be produced, but with dispersant BST will be produced in spindle feature. According to Khollam et al. [55] we can even obtain star-shaped BST powders. The particles of BST are spherical in nature with sizes in the range of 0.8–1.2 μm, but it is expected to obtain good sintering activity since the particles possess sub-

micron powder particle size and surface area of nano-powders [6]. In BSTs produced by solvothermal route the initial Ba/Sr ratio is different from final Ba/Sr ratio, but no dislocation is observed. The particle morphology changes from irregular sphere to polygon, and to cube as the strontium content increases in BST powders produced by this route. It could be achieved, single phase BST by spray pyrolysis with spherical submicronic particles, however in some parts amorphous phase is observed. The produced material has spherical feature but is not well crystallized.

In last method, time of heating did not have such an influence on BST powders [67]. Nanocrystalline $Ba_{0.7}Sr_{0.3}TiO_3$ powder of average size 15 nm could be synthesized via sol-gel route.The relatively fine particle size is the advantage of this route.

ACKNOWLEDGEMENT

We would like to offer our sincere thanks to Young Researchers' Club, Islamic Azad University for supporting this work.

ABBERVIATIONS

2-D: two-dimensional
AFM: atomic force microscope
BST: barium strontium titanate
BSTO: barium strontium titanyl oxalate
CVD: chemical vapor deposition
DIW: de-ionized water
DRAM: dynamic random access memory
DTEM: Dynamic Transmission Electron Microscope
EDS: energy-dispersive spectroscopy
EDX: energy-dispersive X-ray (spectroscopy)
ESAVD: Electrostatic Spray Assisted Vapor Deposition
FWHM: full width at half maximum
HTO: oxalotitanic acid
ICP: Inductively Coupled Plasma
MLCC: multilayer ceramic capacitor
PEG: polyethylene glycol
PLD: pulsed laser deposition
PMAA: poly mathacrylic acid
r.f: radio frequency
RMS: roughness measurement system
SEM: scanning electron microscope
TG: Thermo-Gravimetric
TEM: transmission electron microscopy
TGA/DSC: Thermo-gravimetric analysis / Differential Scanning Calorimetry
UHV: ultrahigh vacuum
wt.%: weight percent
XRD: X-ray diffractometer

REFERENCES

[1] Chang Q. Sun, (2007), Size dependence of nanostructures: Impact of bond order deficiency Progress in *Solid State Chemistry*, 35: 1-159.
[2] A.P. Alivisatos, (1996), Semiconductor clusters, nanocrystals and quantum dots, *Science*, 271: 933-937.
[3] J. Hu, T.W. Odom, C.M. Lieber, (1999), Chemistry and Physics in One Dimension: Synthesis and Properties of Nanowires and Nanotubes , Acc. *Chem. Res*. 32 : 435-445.
[4] L.E. Brus, J.K. Trautman, Philos. Trans. R. Soc. London Ser. (1995) , A-Math Phys. *Eng. Sci*. 353: 313.
[5] J.R. Heath, (1999), Nanoscale Materials, Acc. *Chem. Res*., 32 : 388.
[6] Ming-li Li, Hui Liang, Ming-xia Xu, (2008), Simple oxalate precursor route for the preparation of brain-like shaped barium–strontium titanate: $Ba_{0.6}$ $Sr_{0.4}$ TiO_3, *Mater. Chem. Phys*, 112 : 337-341.
[7] Xiao W, Gang X, Zhaohui R, Yonggang W, Ge S, Gaorong H, (2008), Composition and shape control of single-crystalline Ba_{1-x} Sr_x TiO_3 (x = 0–1) nanocrystals via a solvothermal route, *J. Crystal Growth*, 310 : 4132-4137.
[8] S. Ezhilvalavan, Tseung-Yuen Tseng, (2000), Progress in the developments of (Ba,Sr)TiO_3 (BST) thin films for Gigabit era DRAMs, *Mater. Chem. Phys*, 65: 227-248.
[9] C.M. Carlson, T.V. Rivkin, P.A. Parilla, J.D. Perkins, D.S. Ginley, A.B. Kozyrev, V.N. Oshadchy, A.S. Pavlov, (2000), Large dielectric constant ($\in/\in_0$>6000) $Ba_{0.4}Sr_0.6TiO_3$ thin films for high-performance

microwave phase shifters, *Appl. Phys. Lett*, 76 :1920-1922

[10] F. Zimmermann, M. Voigts, C. Weil, R. Jakoby, P. Wang, W. Menesklou, E. Ivers-Tiffée, (2001), Investigation of barium strontium titanate thick films for tunable phase shifters, *J. Eur. Ceram. Soc*., 21: 2019-2023.

[11] Zhang L., Zhong W.L., Wang C.L., Zhang P.L., Wang Y.G.,(1998), Dielectric relaxation in barium strontium titanate, Solid State Commun. , 107 : 769-773.

[12] R.Li, J.Cheng,Z.Meng,W.Wu, (2006), Low dielectric loss and enhanced tunable properties of Cr- doped barium strontium titanate solid solution, *J.Mater. Sci.Mater.Electron*, 17: 587-591.

[13] Jian Quan Qi, Yu Wang, Wan Ping Chen, Long Tu Li, Helen Lai Wah Chan, (2005), Direct large-scale synthesis of perovskite barium strontium titanate nano-particles from solutions, *Solid State Chem*, 178: 279-284.

[14] Ming-li Li, Ming-xia Xu, (2009), Effect of dispersant on preparation of barium–strontium titanate powders through oxalate co-precipitation method, *Materials Research Bulletin*, 44: 937-942

[15] Seema Agarwal, G. L. Sharma, (2002), Humidity sensing properties of (Ba, Sr) TiO3 thin films grown by hydrothermal–electrochemical method, *Sens. Actuators B*, 85:205-211.

[16] Hongli Guo, Wei Gao, Juhyun Yoo, (2004), The effect of sintering on the properties of $Ba_{0.7}Sr_{0.3}TiO_3$ ferroelectric films produced by electrophoretic deposition, *Mater. Lett*, 58:1387-1391.

[17] J. M. Siqueiros, J. Portelles, S. García, M. Xiao, S. Aguilera, (1999), Study by hysteresis measurements of the influence of grain size on the dielectric properties of ceramics of the $Sr_{0.4}Ba_{0.60}TiO3$ type prepared under different sintering conditions, *Solid State Commun* , 112 : 189-194.

[18] L. C. Sengupta, S.Sengupta, (1997), Novel ferroelectric materials for phased array antennas, IEEE Transactions on Ultrasonics, Ferroelectrics, and Frequency Control, 44 :792-797.

[19] Jr.L. Davis, L.G. Rubin, (1953), Some dielectric properties of barium-strontium titanate ceramics at 3000 megacycles, *J. Appl. Phy*, 24 :1194-1197.

[20] T. Mazon, M.A. Zaghete, J.A. Varela , E. Longo, (2007), Barium strontium titanate nanocrystalline thin films prepared by soft chemical method, *J. Euro. Ceram. Soc*, 27 : 3799-3802.

[21] H.M. Lin, B. Y.Wei, S. F.Pan, , S. C. Tsai, H. F.Lin, (2003), Metallic nanocrystallites-coated piezoelectric quartz for applications in gas sensing, *Journal of Nanoparticle Res*, 5: 157-165.

[22] Yu, H., (2003), Structure and Magnetic Properties of SiO_2 Coated Fe_2O_3 Nanoparticles Synthesized by Chemical Vapor Condensation Process, *Rev. Adv. Mater. Sci*., 4: 55-59.

[23] B. L. Zhu, B. Y. Wei, S. F. Pan, S. C. Tsai, H. F. Lin, (2003), Synthesis and gas sensitivity of In-doped ZnO nanoparticles, *J. Mater. Sci.: Mater. Electron*, 14 : 521-526.

[24] Thomas K. H. Starke, Gary S. V. Coles, (2003), Laser-ablated nanocrystalline SnO_2 material for low-level CO detection, *Sensor Actuator B*, 88: 227-233.

[25] Xi Li, Fabin Qiu, Kui Guo, Bo Zou, Jianmin Gu, Jing Wang, Baokun Xu, (1997), Synthesis and humidity sensitive properties of nanocrystalline $Ba_{1-x}Sr_xTiO_3$ thick films, *Mater.Chem.phys*, 50: 227-232.

[26] O. P. Thakur, Chandra Prakash, D. K. Agrawal, (2002), Microwave synthesis and sintering of $Ba_{0.95}Sr_{0.05}TiO_3$, *Mater.Lett*, 56: 970-973.

[27] Di Wu, Aidong Li, Huiqin Ling, Xiaobo Yin, Chuanzhen Ge, Mu Wang, Naiben Ming, (2000), Preparation of $(Ba_{0.5}Sr_{0.5})TiO_3$ thin films by sol–gel method with rapid thermal annealing, *Appl. Surf. Sci*, 165:309-314.

[28] S.B. Deshpande, Y.B. Khollam, S.V. Bhoraskar, S.K. Date, S.R. Sainkar, H.S. Potdar, (2005), Synthesis and characterization of microwave-hydrothermally derived $Ba_{1-x}Sr_xTiO_3$ powders, *Mater. Lett*, 59:293-296.

[29] G. Branković, Z. Branković, M.S. Góes, C.O. Paiva-Santos, M. Cilense, J.A. Varela, E. Longo, (2005), Barium strontium titanate

powders prepared by spray pyrolysis, *Mater. Sci. Eng. B*, 122: 140-144.

[30] T. V. Anuradha, S. Ranganathan, Tanu Mimani, K. C. Patil, (2001), Combustion synthesis of nanostructured barium titanate, *Scripta. Mater*, 44: 2237-2241.

[31] Zhimin Zhong, Patrick K. Gallagher, (1995), Combustion synthesis and characterization of $BaTiO_3$, *J. Mater. Res*, 10:942-952.

[32] Schrey, F.,(1965),Effect of pH on the Chemical Preparation of Barium-Strontium Titanate, *J. Am. Cer. Soc*. 48:401-405.

[33] Y.B. Khollam, S.B. Deshpande, H.S. Potdar, S.V. Bhoraskar, S.R. Sainkar, S.K. Date, (2005), Simple oxalate precursor route for the preparation of barium–strontium titanate: $Ba_{1-x}Sr_xTiO_3$ powders, *Mater. Charact*, 54: 63-74.

[34] Huang Jiquan, Hong Maochun, Jiang Feilong, Cao Yongge, (2008), Synthesis of nanosized perovskite (Ba,Sr)TiO_3 powder via a PVA modified sol-precipitation process, *Mater. Lett*, 62: 2304-2306.

[35] Jing Du, Kwang-Leong Choy, (2006), Fabrication and structural characterization of (Ba,Sr)TiO_3 thin films produced by Electrostatic Spray Assisted Vapour Deposition, *Mater. Sci. Eng. C*, 26: 1117-1121.

[36] Y.G. Sun, Y.N. Xia, (2002), Shape-controlled synthesis of gold and silver nanoparticles, *Science*, 298: 2176-2179.

[37] X. G. Peng, L. Manna, W.D. Yang, J. Wickham, E. Scher, A. Kadavanich, A.P. Alivisatos, (2000), Shape control of CdSe nanocrystals, *Nature*, 404: 59-61.

[38] J.I. Clark, T. Takeuchi, N. Ohtori, D.C. Sinclair, (1999), Hydrothermal synthesis and characterization of BaTiO3 fine powders: Precursors, polymorphism and properties, *J. Mater. Chem*, 9: 83-91.

[39] Bharat L. Newalkar, Sridhar Komarneni, Hiroaki Katsuki, (2001), Microwave-hydrothermal synthesis and characterization of barium titanate powders, *Mater. Res. Bull*, 36: 2347-2355.

[40] A. Ries, A. Z. Simões, M. Cilense, M. A. Zaghete, J. A. Varela, (2003), Barium strontium titanate powder obtained by polymeric precursor method, *Mater. Charact*, 50: 217-221.

[41] P. Pinceloup, C. Courtois, A. Leriche, B. Thierry, (1999), Hydrothermal synthesis of nanometer sized barium titanate powders: control of barium/titanium ratio, sintering, and dielectric properties, *J. Am. Ceram. Soc*, 82: 3049–3056

[42] R.K. Roeder, E.B. Slamovich, (1999), Stoichiometry control and phase selection in hydrothermally derived Ba_xSr_{1-x} TiO_3, *J. Am. Ceram. Soc*, 82:1665–1675.

[43] S.B. Deshpande, Y.B. Khollam, S.V. Bhoraskar, S.K. Date, S.R. Sainkar, H.S. Potdar, (2005), Synthesis and characterization of microwave-hydrothermally derived Ba_{1-x} Sr_xTiO_3 powders, *Mater. Lett* , 59: 293–296.

[44] S.-F. Liu, I.R. Abothu, S. Komarneni, (1999), Barium titanate ceramics prepared from conventional and microwave hydrothermal powders, *Mater. Lett* , 38: 344–350.

[45] K.A. Razak, A. Asadov, W. Gao, (2007), Properties of BST ceramics prepared by high temperature hydrothermal process, *Ceramics International*, 33: 1495-1502.

[46] Liu S.-F., Abothu I.R., Komarneni S.,(1999) Barium titanate ceramics prepared from conventional and microwave hydrothermal powders, *Mater. Lett.*, 38: 344-350.

[47] Sylvia Koerfer, Roger A. De Souza, Han-Ill Yoo, Manfred Mart, (2008), Diffusion of Sr and Zr in $BaTiO_3$ single crystals, *Solid State Sciences*, 10: 725-734.

[48] A.I. Kingon, J.P. Maria, S.K. Streiffer, (2000), Alternative dielectrics to silicon dioxide for memory and logic devices, *Nature*, 406: 1032-1038.

[49] Naoto Koshizaki, Aiko Narazaki, Takeshi Sasaki, (2002), Preparation of nanocrystalline titania films by pulsed laser deposition at room temperature, *Appl. Surf. Sci*, 197:624-627.

[50] Seng Lu Yang, Jenn Ming Wu, (1995), Effects of Nb_2O_5 in (Ba,Bi,Nb)-added TiO_2 ceramic varistors, *J. Mater. Res*, 10: 345-352.

[51] J. Moon, J. A. Kerchner, H. Krarup, J. H. Adair, (1999), Particle-shape control and formation mechanisms of hydrothermally derived lead titanate, *J. Mater. Res*., 14: 866-875.

[52] J. Moon, J. A. Kerchner, H. Krarup, J. H. Adair, (1999), Hydrothermal synthesis of ferroelectric perovskites from chemically modified titanium isopropoxide and acetate salts, *J. Mater. Res*,14: 425-435.

[53] Patrick K. Gallagher, Frank Schery, Frank V. Dimarcello, (1963), Preparation of Semiconducting Titanates by Chemical Methods, *J. Am. Ceram. Soc*. 46 : 359-365.

[54] P.K. Gallagher, F. Schrey, (1963),Thermal Decomposition of Some Substituted Barium Titanyl Oxalates and Its Effect on the Semiconducting Properties of the Doped Materials, *J. Am. Ceram. Soc*. 46 : 567-573.

[55] Y. B. Khollam, H. S. Potdar , S. B. Deshpande, A. B. Gaikwad, (2006), Synthesis of star shaped $Ba_{1-x}Sr_xTiO_3$ (BST) powders, *Mater. Chem. Phys*, 97: 295-300.

[56] R.K. Roeder, E.B. Slamovich, (1999), Stoichiometry control and phase selection in hydrothermally derived $Ba_xSr_{1-x}TiO_3$ powders,, *J. Am. Ceram. Soc*, 82: 1665-1675.

[57] J. Moon, E. Suvaci, A. Morrone, S.A.. Costantino, J.H. Adair, (2003), Formation mechanisms and morphological changes during the hydrothermal synthesis of $BaTiO_3$ particles from a chemically modified, amorphous titanium (hydrous) oxide precursor, *J. Eur. Ceram. Soc*, 23: 2153-2161.

[58] JCPDS No. 74-1968, JCPDS No. 39-1395, JCPDS No. 79-0176.

[59] L. Qi, B.I. Lee, P. Badheka, D.H. Yoon, W.D. Samuels, G.J. Exarhos, (2004), Short-range dissolution-precipitation crystallization of hydrothermal barium titanate, *J. Eur. Ceram. Soc*, 24 : 3553-3557.

[60] P.K. Sharma, V.V. Varadan, V.K. Varadan, (2000),Porous behavior and dielectric properties of barium strontium titanate synthesized by sol-gel method in the presence of triethanolamine, *Chem. Mater*, 12: 2590-2596.

[61] W. Nimmo, N.J. Ali, R.M. Brydson, C. Calvert, E. Hampartsoumian, D. Hind, S.J. Milne, (2003), Formation of lead zirconate titanate powders by spray pyrolysis, *J. Am. Ceram. Soc* ,86: 1474-1480.

[62] G.H. Haertling, (1999), Ferroelectric ceramics: History and technology, *J. Am. Ceram. Soc*, 82: 797-818.

[63] G. Brankovic, Z. Brankovic, M.S. Goes, C.O. Paiva-Santos, M. Cilense, J.A. Varela, E. Longo, (2005) , Barium strontium titanate powders prepared by spray pyrolysis, *Mater. Sci. Eng. B*, 122 :140–144.

[64] T.T. Kodas, (1989) Generation of Complex Metal Oxides by Aerosol Processes: Superconducting Ceramic Particles and Films,, Angew., *Chem. Int. Ed. Engl*., 28 : 794-806.

[65] L.W. Finger, D.E. Cox, A.P. Jephcoat, (1994), A correction for powder diffraction peak asymmetry due to axial divergence, *J. Appl. Crystallogr*. 27: 892-902.

[66] K.L. Choy, (2001) , Processing–structure–property of nanocrystalline materials produced using novel and cost-effective ESAVD-based methods,Mater. Sci. Eng., C, Biomim. *Mater., Sens. Syst*. 16 : 139-145.

[67] D. Hennings, S. Schreinmacher, (1992), Characterization of hydrothermal barium titanate, *J. Eur. Ceram. Soc*. 9 : 41-46.

[68] V. Somani , S. J. Kalita, (2007), Synthesis and characterization of nanocrystalline Barium Strontium Titanate powder via sol-gel processing , *J. Electroceram* 18: 57-65.

[69] P.K. Sharma, V.V. Varadan, V.K. Varadan, (2000), Porous Behavior and Dielectric Properties of Barium Strontium Titanate Synthesized by Sol−Gel Method in the Presence of *Triethanolamine*, *Chem. Mater*. 12: 2590-2596.